Millimeter and submillimeter wave spectroscopy of propanal

Oliver Zingsheim[a,*], Holger S.P. Müller[a], Frank Lewen[a], Jes K. Jørgensen[b], Stephan Schlemmer[a]

[a]*I. Physikalisches Institut, Universität zu Köln, Zülpicher Str. 77, 50937 Köln, Germany*
[b]*Centre for Star and Planet Formation, Niels Bohr Institute and Natural History Museum of Denmark, University of Copenhagen, Øster Voldgade 5–7, 1350 Copenhagen K, Denmark*

Abstract

The rotational spectra of the two stable conformers *syn*- and *gauche*-propanal (CH_3CH_2CHO) were studied in the millimeter and submillimeter wave regions from 75 to 500 GHz with the Cologne (Sub-)Millimeter wave Spectrometer. Furthermore, the first excited states associated with the aldehyde torsion and with the methyl torsion, respectively, of the *syn*-conformer were analyzed. The newly obtained spectroscopic parameters yield better predictions, thus fulfill sensitivity and resolution requirements in new astronomical observations in order to unambiguously assign pure rotational transitions of propanal. This is demonstrated on a radio astronomical spectrum from the Atacama Large Millimeter/submillimeter Array Protostellar Interferometric Line Survey (ALMA-PILS). In particular, an accurate description of observed splittings, caused by internal rotation of the methyl group in the *syn*-conformer and by tunneling rotation interaction from two stable degenerate *gauche*-conformers, is reported. The rotational spectrum of propanal is of additional interest because of its two large amplitude motions pertaining to the methyl and the aldehyde group, respectively.

Keywords:
propanal, rotational spectroscopy, submillimeter wave spectroscopy, interstellar molecule, internal rotation, tunneling rotation interaction

1. Introduction

In 1964, Butcher and Wilson recorded the microwave spectrum of propanal, also known as propionaldehyde, and deuterated isotopic species up to 38 GHz. The existence of two stable conformers, *syn* (also called *cis*) and the doubly-degenerate *gauche* conformer (from here on simply *syn* and *gauche*) was established [1]. A sketch of *syn* is shown in Fig. 1. The two conformers differ mainly by the rotation of the aldehyde group with respect to the carbon atom plane of the molecule. Furtheron transitions in low-lying excited vibrational states were also identified [1]. The potential energy surface of the rotation of the aldehyde group was studied in detail later [2, 3]. It was found that *gauche* is higher in energy by ~420 cm^{-1} and the aldehyde group is rotated by ±128.2° compared to the *syn* orientation [3]. The potential energy surface of propanal with respect to the rotation of the aldehyde group and sketches of the conformers are shown in Fig. 2. The torsional potentials were determined more accurately by Far-IR spectroscopy [4] and higher-lying vibrational modes were studied by Mid-IR spectroscopy [5]. In particular, the first aldehyde torsion $v_{24} = 1$ is 135.1 cm^{-1} and the first excited methyl torsion $v_{23} = 1$ is 219.9 cm^{-1} above the ground state of *syn* [4]; note that the methyl torsional assignments have been exchanged between *syn* and *gauche* from Ref. [4] to Ref. [5]. In the former work the energy difference between the conformers was redetermined as
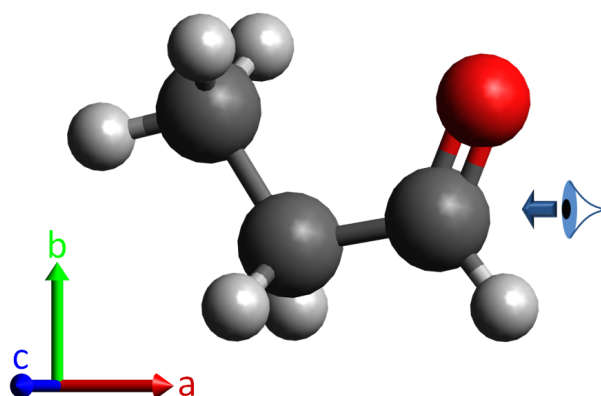

Figure 1: Sketch of *syn* propanal, CH_3CH_2CHO. White spheres designate hydrogen, black ones carbon, and the red one oxygen atoms. All heavy atoms, three carbon and one oxygen, are in the *ab*-plane.

~421 cm^{-1}, whereas in the latter work it was determined to be ~370 cm^{-1}.

Whereas the rotational spectrum of *syn* displays only small splittings caused by an internal rotation of the methyl group, the barrier between the two equivalent *gauche* conformations is sufficiently low (see Fig. 2) such that tunneling between them occurs, causing somewhat larger splittings [1].

Two groups measured further transitions of *syn* independently of each other in the frequency region from 8–38 GHz using a Stark-modulated and a Fourier transform microwave

---

*Corresponding author.
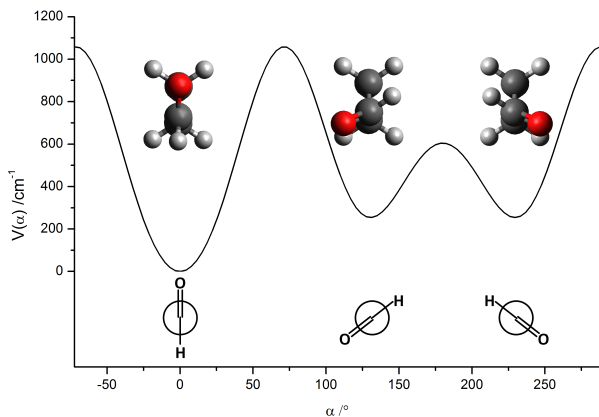Email address:* zingsheim@ph1.uni-koeln.de (Oliver Zingsheim)

Figure 2: Calculated potential energy surface of propanal with respect to the rotation of the aldehyde group [4]. There are two stable conformers: *Syn-* and the twofold degenerate *gauche*-conformer. White spheres in propanal sketches designate hydrogen, black ones carbon, and red ones oxygen atoms. The molecular axes *c* and *b* are aligned to the *x*- and *y*-axis, respectively. The point of view is shown for *syn* with the eye in Fig. 1. Since *syn* and *gauche* conformers differ mainly by the rotation of the aldehyde group, this alignment was chosen for clarification. Their simplified Newman projections, where the three carbon atoms are shown as one cycle and hydrogen atoms are omitted, except the one from the aldehyde group, are highlighting this rotation. A more illustrative alignment of *syn* is shown in the supplementary material.

spectrometer, respectively, but published it jointly [6]. They used a *S*-type centrifugal distortion analysis to guarantee a correct assignment of transitions involving states of large angular momentum *J*. Additionally, the height of the methyl barrier hindering internal rotation in *syn* was determined to ~793.7 cm^{-1}. For *gauche* it is ~886 cm^{-1} and was determined by measuring *c*-type transitions [7]. This was crucial since *b*- and *c*-type transitions were predicted to split by internal rotation and only *a*-types were assigned before [1, 2]. Assignment of rotational transitions for *syn* were extended nearly up to 300 GHz with a spectrometer employing super-heterodyne detection [8]. Structural information on either conformer were derived from twelve isotopologues of *syn* and six of *gauche* [9].

In the homologous series of alkanales, the three smallest members, methanal, ethanal, and propanal were already detected in space [10, 11, 12]. The first detection of propanal was towards Sgr B2(N) [12]. Later, it was detected also in other galactic center molecular clouds [13] and very recently in the Protostellar Interferometric Line Survey (PILS) [14] of the low-mass protostellar binary IRAS 16293−2422 [15] using the Atacama Large Millimeter/submillimeter Array (ALMA). The first two detections indicated that the molecule is located in colder environments, whereas the most recent one is in a comparably warm one at around 125 K. Its detection is in the warm gas close to the protostar, where molecules desorb from the grain ice mantle and the column density is high. The lines toward one component in IRAS 16293−2422 are very narrow, approximately 1 kms^{-1} wide, and the PILS data indicated small discrepancies between some observed and predicted rotational lines of propanal [15]. The discrepancies may arise in part from the complexity of the astronomical spectrum itself, es-

pecially from presently unaccounted absorption lines affecting the emission lines. Furthermore, some of the lines in the observed frequency region (329−363 GHz) had non-negligible uncertainties. Finally, the identification of propanal in the survey was based on predictions which had ignored the small, often unresolved internal rotation splitting. Since higher accuracies are desired, especially in higher frequency regions, and propanal was also found in a warmer environment, the spectrum of propanal was measured from 75 up to 500 GHz at room temperature with the Cologne (Sub-)Millimeter wave spectrometer and analyzed with respect to the splittings of the lines and its energetically lowest lying vibrational states. Another incentive for us to revisit the rotational spectrum of propanal was the presence of the two large amplitude vibrations and their potential interaction. In the current work, we present results on the ground vibrational states of *syn* and *gauche* and the first excited aldehyde and methyl torsional states of *syn*.

2. Experimental details

The spectrum of propanal was measured continuously in the frequency regions of 75−129 GHz and 169.2−500.4 GHz with the Cologne (Sub-)Millimeter wave Spectrometer. The experimental setup is described in detail elsewhere [16]. In this work, a clean pyrex cell was used. A rooftop mirror was installed at one end of the 5 m long cell with a diameter of 10 cm to double the absorption path length. For covering the 75−129 GHz range, in-house developed electronics for operating an amplifier tripler chain (~10 mW) in full saturation mode and a low noise room temperature Schottky detector were used to improve the signal to noise ratio (SNR). The higher frequency range was operated with commercial multiplier chains [17]. Typical background pressures (vacuum) reached 0.1 µbar and the cell was filled with a commercially available sample of propanal (97 %) from Sigma-Aldrich to a total pressure of about 20 µbar (2 Pa). Frequency modulation (FM; ~50 kHz, amplitude usually between 180 and 300 kHz) was employed with 2*f* demodulation which causes isolated absorption signals to appear close to a second derivative of a Gaussian. The step size varied between 81 and 108 kHz, and the integration time was usually 50 ms. Approximately two gigahertz could be measured per hour. We assigned uncertainties of 20 kHz to strong and very symmetric lines, 40 or 80 kHz to weaker or less symmetric lines.

3. Spectroscopic analysis

The rotational spectrum of propanal is very rich even at the lowest frequencies of our study. In Figure 3, observed lines of ground vibrational states of *syn* and *gauche* and the first excited aldehyde and methyl torsional states of *syn* are shown. Even though spectra are quite dense, unambiguous assignments can be made. In general, intensity ratios and trends in deviations of observed and calculated lines for different series were used to unambiguously assign transitions to the observed lines. In fact, in the higher frequency region, this high density of lines is restraining our assignments for lines with large uncertainties
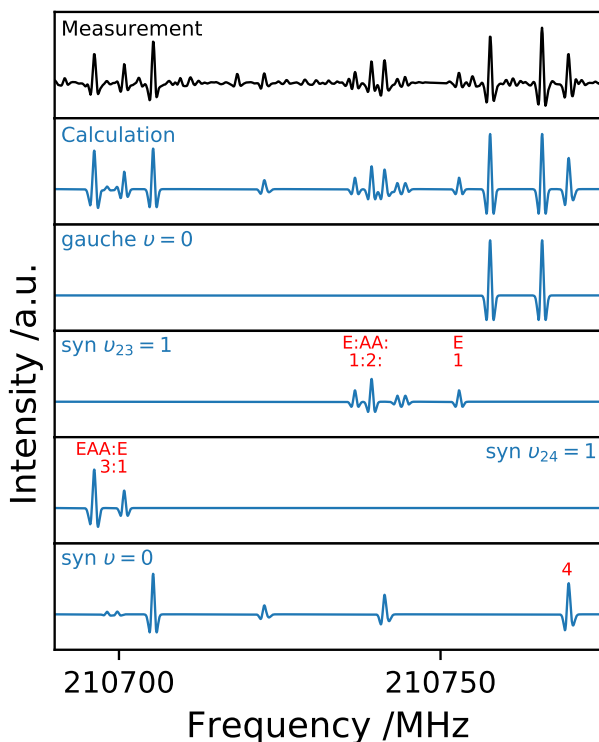
Figure 3: In the top panel is the measured spectrum of propanal around 210.7 GHz in black in order to show various contributions of the states studied in this work. Beneath is in blue the calculated spectrum including, also shown separately in blue from the bottom panel upwards, synthetic spectra of the ground state ($v = 0$), first excited aldehyde ($v_{24} = 1$) as well as first excited methyl torsion ($v_{23} = 1$) of *syn* and the ground state of *gauche*. Resulting A and E lines due to internal rotation in *syn* can be blended or be separated. For *R*-type *a*-type transitions additional asymmetry splitting with $K_a + K_c = J$ and $K_a + K_c = J + 1$ could be observed. These 4 transitions are frequently blended for higher J values. Exemplary (in red) different intensity ratios are shown. In the ground state all 4 lines are blended for $J' = 20$ and $K_a = 17$, in $v_{24} = 1$ a 3:1 ratio is observed for $J' = 20$ and $K_a = 10$, and a 1:2:1 ratio for $v_{23} = 1$ for $J' = 20$ and $K_a = 11$. Asymmetric lineshapes appear if transitions are not completely merged, yet unresolved. Unassigned lines belong to further vibrationally excited states, isotopologues and possible impurities in the cell.

more often than limitations in the signal-to-noise ratio. Figures 3 and 4 already give a hint of the line confusion, however they were choosen to clarify different aspects of the spectra, so there are much more crowded frequency regions. Thus far, about 15 % of the observed lines could be assigned to the ground states of both conformers and to the two lowest vibrationally excited states of *syn*.

3.1. syn-propanal

The lower energy *syn* conformer is an asymmetric top rotor with $\kappa = -0.7855$ in the ground vibrational state (prolate case: $\kappa = -1$). The dipole moment components of *syn* were determined from Stark-effect measurements as 1.71 D and 1.85 D along the *a*- and *b*-axis, respectively [1]. The *c*-component is zero owing to the C_S-symmetry of the conformer. Rotational lines may be split into A and E components with equal intensities due to the threefold degenerate potential of the methyl

group for internal rotation. A full description of molecular symmetry, with symmetry tables for the rigid rotor assumption and allowing for internal rotation, as well as resulting energy levels and selection rules can be found in the supplementary material.

In general, for all studied *syn* states, lines in a frequency window of ~30 GHz were assigned and then a new fit was performed, if necessary with additional parameters. In general, intensity ratios and trends in deviations of observed and calculated lines for different series were used to unambiguously assign transitions to the observed lines. With improved parameters, a prediction for the next frequency window was made and so on. Indeed, for both vibrationally excited states only limited microwave data were available. Thus assignments in the millimeter wave range were more challenging. Due to no overlapping frequency regions from literature and our spectra, centrifugal distortion constants were kept fixed to the ground state values as a starting point. In a first step, the rotational parameters *A*, *B*, *C*, and the energy tunneling parameter ϵ_{10} were fit to the literature data. Subsequently, strong and well separated lines could be assigned for the first few gigahertz. Improved centrifugal distortion constants led to improved predictions especially for lines slightly higher in *J* or in K_a.

Groner's ERHAM program [18] was used for predicting and fitting of the rotational spectrum, including splittings due to internal rotation (for the ground vibrational state an extended version was used, since the original version is limited to 8191 transitions). To calculate an initial unitless internal rotation parameter ρ and the angle Θ_{RAM} for applying the Rho-Axis Method (RAM), the formulas $\rho_g = \lambda_g I_\alpha / I_g$ and $\Theta_{RAM} = arctan(\rho_b/\rho_a)$ were used ($g = a, b, c$) [19]. The direction cosines of the internal rotation axis *i* of the top in the principal axis system λ_g, moments of inertia I_g, and moment of inertia of the top I_α were taken or calculated with rotational parameters and the angle $\sphericalangle(a, i)$ from the literature [6], resulting in $\rho = 0.06$ and $\Theta_{RAM} = 28°$.

The ground vibrational state shows only small, whereas excited vibrational states show larger splittings. Hence, the ratio of observed lines to assigned transitions is higher for vibrationally excited states (specifically, ground state transitions are more frequently blended) and more tunneling parameters are required to reproduce the data within experimental uncertainties. In Table 1, rotational and tunneling parameters of the ground state and first excited aldehyde-torsion as well as first excited methyl-torsion of *syn* are listed.

3.1.1. the ground state, $v = 0$ ($E = 0 \, cm^{-1}$)

Starting with the ground state of *syn*-propanal at 75 GHz, assignments were more or less straightforward, since some transitions were already measured and assigned up to 290 GHz. Great care had to be taken into account with some typos and bad lines from the literature, conspicuously large deviations from experimental to calculated frequencies. For example, the A and E components of transition $6_{4,2} - 5_{3,3}$ were listed at 145035.5 GHz, whereas we predict this line at 143035.5 GHz, shifted by 2 GHz. Since the bad lines were unknown at this point and due to a large overlap from literature data and ours, transitions from Ref. [8] were completely excluded from the fit

after first assignments were done in the millimeter wave range. In the end, these 112 lines (with corrected typos) were included in an additional fit and only four show larger deviations, see supplementary material. One of them is the line mentioned above, for the other three lines the splitting due to internal rotation was neglected. Due to comparably strong dipole moment components along the a- and b-axis, mostly a- and b-type R- and Q-type transitions were assigned ($a - R$: 2963, $a - Q$: 542, $b - R$: 1567, $b - Q$: 2832, $b - P$: 4). ERHAM also labels some transitions as false (arising from mislabeling) or "forbidden" (mixed wavefunctions, i.e., when the tunneling splitting is approximately equal to the torsional splitting) c-type R- (186), Q- (163), and P-type (23) transitions plus 271 so called x-type P-type transitions, see Ref. [20]. In general, energy levels with higher angular momentum J show smaller splittings for identical K's. The b-type transitions with low J and high K_a are frequently split; splitting in a-type transitions was resolved for R-type transitions with large asymmetry splitting ($2K_a \approx J$) and lower values of J. The root mean square (RMS) error of the fit was quite constant up to 300 GHz. The deterioration of the fit quality with higher frequency assignments, up to ~20 %, was ameliorated with the inclusion of L_{KKJ}.

3.1.2. the 1st excited aldehyde torsion, $v_{24} = 1$ ($E = 135.1\,cm^{-1}$)

In general, assignments and fitting were nearly straightforward for the first excited aldehyde torsion, similar to the ground state. Noticeable is that series of b-type transitions, with higher K_a quantum numbers than were already implemented in the fit, needed to be weighted carefully step by step into the dataset. Sometimes, this was also observed in the ground state, albeit to a lesser extent. With a sufficient amount of new lines these transitions were fit satisfactorily, and assignments in the submillimeter wave region could be made. Eventually, all assigned lines from the first excited aldehyde torsion could be fit within experimental uncertainty.

3.1.3. the 1st excited methyl torsion, $v_{23} = 1$ ($E = 219.9\,cm^{-1}$)

Assignment and fitting of transitions within the first excited methyl torsion of *syn* turned out to be much more complicated. First, observed lines are weaker, so lines are more frequently blended and, due to many weak lines in the spectra, special care had to be taken into account to avoid misassignments. Furthermore, larger splittings due to internal rotation hampered assignments by finding patterns. We have not been able to fit all assigned lines within experimental uncertainties. Nevertheless, out of the 3688 assigned transitions 2760 were reproduced satisfyingly. The observed deviations may originate from incorrect assignments, however, the discontinuities in our dataset are evidence of perturbed rotational energy levels. For example, an oblate pairing of transitions is observed for high J values with $K_a = 3$, 4, and lines can be assigned up to $J_{max} = 51$. In the final fit lines with $J = 39 - 46$ are excluded and show deviations up to 5 MHz.

The present model treats the $v_{23} = 1$ (A'' symmetry) state as isolated. However, its energy of 219.9 cm^{-1} [4, 5] is not only comparable to $v_{24} = 2$ at 269.3 cm^{-1}, the second excited state

of the aldehyde torsion (A'), but also to the A' CCC-bending fundamental $v_{15} = 1$ at 264.0 cm^{-1} [4, 5]. Thus, Coriolis interaction may occur between $v_{23} = 1$ and $v_{15} = 1$. In addition, rotational or Coriolis-type interaction may occur between $v_{23} = 1$ and $v_{24} = 2$, which is most likely less prominent because it is of higher order than the Coriolis interaction between two fundamentals, besides, $v_{24} = 2$ is farther away from $v_{23} = 1$ than is $v_{15} = 1$. The analysis likely becomes even more complex because of a possible Fermi resonance between $v_{15} = 1$ and $v_{24} = 2$.

As usual, the value of J_{max} used in the fit is almost always decreasing for transitions involving energy levels with increasing K_a quantum numbers. For $K_a = 0$, J_{max} is 54, whereas for $K_a = 16$ it is 19. Excluded lines with higher quantum numbers are still unweighted in the fit file, but need to be treated with caution, considering that a proper treatment of interactions could lead to new assignments, since frequencies can be shifted up to several megahertz, and the spectra are crowded with lines. In this case, a new fit was performed by starting from scratch and increasing J and K_a step by step, with no improvement. A full treatment of interactions could enable to include all assigned lines in the future.

3.2. ground state of gauche-propanal, $v = 0$ ($E \approx 370\,cm^{-1}$)

The higher energy *gauche* conformer is an asymmetric top rotor with $\kappa = -0.9849$ quite close to the limiting prolate case. It is doubly-degenerate with C_1 symmetry. The low barrier between the two equivalent minima facilitates tunneling between them, lifting the degeneracy and creating a symmetric and an antisymmetric tunneling state which are often designated as 0^+ and 0^-, respectively. Since a non-vanishing transition dipole matrix element $\langle \psi_i \mid \mu_x \mid \psi_j \rangle$ is mandatory to observe a rotational transition, the wave functions ψ_i and ψ_j need to have the same symmetry for a- and b-type transitions ($x = a, b$). Hence, these transitions only occur within substates 0^+ and 0^-. However, the direction of μ_c is changing for the left and right handed version, for that reason c-type transitions occur between substates. The dipole moment components were determined as $\mu_a = 2.645(5)\,D$, $\mu_b = 0.417(6)\,D$, and $\mu_c = 1.016(3)\,D$, respectively [3]. The rotational spectrum of *gauche* with its Coriolis-type interactions was fit and predicted with Pickett's SPFIT and SPCAT programs [21] and using Pickett's reduced axis system [22]. We determined linear combinations of spectroscopic parameters X^+ and X^- from the two substates, explicitly $X = (X^+ + X^-)/2$ and $\Delta X = (X^+ - X^-)/2$, see, e.g., Refs. [23, 24].

The two tunneling states may interact via Coriolis-type interaction of a- or b-type symmetry with the leading coefficients F_{bc} and F_{ac}, respectively. The former connects in particular the upper energy asymmetry component of a given J and K_a with the lower energy asymmetry component of the same J and K_a. The strongest interactions occur for $K_a = 1$, $K_a = 2$, $K_a = 3$, $K_a = 4$, and $K_a = 5$ at $J = 2$, $J = 10$, $J = 22$, $J = 36$, and $J = 52$, respectively. Transitions involving these states are well described in our model. Due to a mixing of energy levels from 0^+ and 0^- substates, also formal x-type transitions (ΔK_a and ΔK_c even) between these states are observed. The operator

Table 1: Spectroscopic parameters[a] (MHz) of the ground state ($v = 0$), first excited aldehyde ($v_{24} = 1$) as well as first excited methyl torsion ($v_{23} = 1$) of *syn*-propanal.

	Parameter	$v = 0$	$v_{24} = 1$	$v_{23} = 1$
	A	16669.626420 (154)	16712.057839 (167)	16642.87187 (61)
	B	5893.503711 (49)	5857.196275 (49)	5871.180340 (171)
	C	4598.982111 (48)	4595.250184 (50)	4592.798935 (116)
	$\Delta_K \times 10^3$	50.06225 (63)	49.70451 (84)	43.9445 (37)
	$\Delta_{JK} \times 10^3$	-19.370540 (153)	-18.097558 (232)	-17.5153 (34)
	$\Delta_J \times 10^3$	5.354247 (37)	5.236678 (38)	5.223946 (211)
	$\delta_K \times 10^3$	4.211646 (164)	3.22843 (30)	1.6032 (32)
	$\delta_J \times 10^3$	1.5662438 (66)	1.5132959 (108)	1.527602 (94)
	$\Phi_K \times 10^9$	986.40 (80)	1070.36 (179)	-221.1 (104)
	$\Phi_{KJ} \times 10^9$	-606.15 (37)	-577.21 (64)	143.2 (109)
	$\Phi_{JK} \times 10^9$	77.271 (65)	62.316 (141)	-128.2 (92)
	$\Phi_J \times 10^9$	2.1239 (88)	2.0061 (92)	0.827 (124)
	$\phi_K \times 10^9$	292.50 (58)	0.03746 (138)	-1.471 (46)
	$\phi_{JK} \times 10^9$	27.236 (49)	25.349 (112)	138.8 (57)
	$\phi_J \times 10^9$	1.49907 (138)	1.28486 (267)	0.555 (62)
	$L_K \times 10^{12}$	–	-79.43 (120)	–
	$L_{KKJ} \times 10^{12}$	14.082 (239)	21.93 (41)	–
	$L_{JK} \times 10^{12}$	–	-4.736 (160)	–
	$L_{JJK} \times 10^{12}$	–	–	-71.7 (56)
	$l_{KJ} \times 10^{12}$	–	–	-809 (32)
	$l_{JK} \times 10^{12}$	–	–	-16.49 (272)
	ϵ_{10}	-3.0942 (57)	38.7984 (68)	130.5541 (250)
	$\epsilon_{20} \times 10^3$	–	–	68.4 (71)
	$[A - (B + C)/2]_{10} \times 10^3$	–	-2.477 (33)	-7.887 (224)
	$[(B + C)/2]_{10} \times 10^3$	–	-0.7392 (62)	-3.761 (38)
	$[(B - C)/4]_{10} \times 10^3$	0.09286 (194)	-1.1251 (80)	-3.8450 (229)
	$\Delta_{K_{10}} \times 10^6$	–	–	-10.80 (65)
	$\Delta_{JK_{10}} \times 10^6$	–	1.1215 (216)	8.83 (38)
	$\delta_{J_{10}} \times 10^6$	–	0.1903 (33)	0.4833 (83)
	$d_{2_{10}} \times 10^6$	–	0.26299 (269)	0.5194 (56)
	$h_{1_{10}} \times 10^{12}$	–	-29.11 (97)	–
	$h_{2_{10}} \times 10^{12}$	–	-16.082 (245)	–
	$G_{z_{10}} \times 10^3$	–	14.82 (31)	67.0 (33)
	$\rho^b \times 10^3$	65.681 (116)	63.8032 (90)	61.9026 (102)
	$\Theta_{RAM}[°]$	27.871 (60)	28.5299 (48)	28.4352 (82)
Combined fit	no. of lines	3901	5084	2085
	no. of transitions	8551	6823	2760
	rms error[b]	0.94	0.93	1.06

[a]Watson's A reduction in the I^r representation was used in ERHAM. Numbers in parentheses are one standard deviation in units of the least significant figures. In the first block are rotational constants, in the second ERHAM tunneling parameters (in Watson's S reduction), and in the last are general information about the fits.
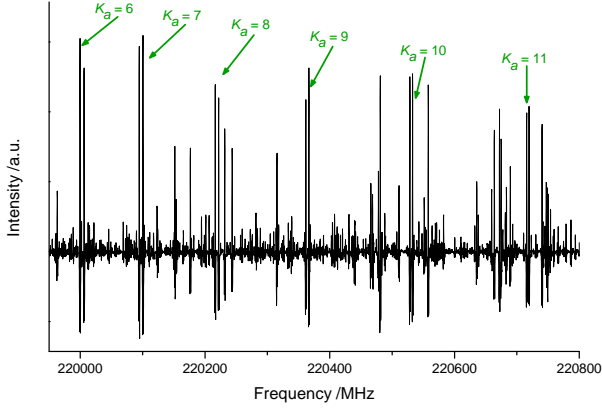[b]Weighted unitless value for the entire fit.

Figure 4: The measured spectrum of propanal around 220 GHz. Labeled here is a set of doublets originating from tunneling rotation interaction from two stable degenerate *gauche*-conformers. The *R*-type *a*-type transitions $26_{K_a, K_c} - 25_{K_a, K_c-1}$ are marked with their respective K_a quantum numbers. The asymmetry splitting ($J = K_a + K_c$ and $J + 1 = K_a + K_c$) is unresolved. The intensities are decreasing with increasing K_a's. The strong lines illustrate the possibility of secure assignments of transitions even with higher K_a quantum numbers. Furtheron the density of lines in the measured spectrum is visible, even though this frequency region was choosen for clarification of the doublet pattern, i.e. there are much more crowded regions full of lines with comparable intensities.

with the F_{ac} coefficient may connect levels of the same J with K_a and K_c differing by an odd number. We did not have clear evidence for this type of interaction.

A splitting due to internal rotation of the methyl group was not observed in the present investigation.

Unfortunately, only *a*-type transitions could be assigned with confidence in our observed spectra, since intensities are proportional to the square of the dipole moment, and *gauche* is in general less populated than *syn* owing to Boltzmann statistics. The *b*-type transitions are by far too weak to be observed, but *c*-type transitions may have sufficient intensity to identify them in the spectrum. We found evidence for a *Q*-type series with $K_a' - K_a'' = 5 - 4$, but the intensities of these lines were in some occasions too weak to assign them securely. Two *Q*-type *b*-type and one *R*-type *c*-type transition from the literature are unweighted in the fit due to conspicuously large deviations.

The fitting procedure was very different for *gauche* compared to *syn*. We started to fit all transitions with $K_a = 0$ up to $J = 45$, followed by series with $K_a = 1$, then $K_a = 2$, and so on. Later, transitions involving J up to 60 were added. To assign and especially to fit transitions, originating in strongly perturbed energy levels, was quite challenging. For $K_a = 2$, transitions from unperturbed energy levels with higher J quantum numbers were implemented earlier in the fit than those from perturbed ones. Otherwise the quality of the fit was too poor. It is possible that the fit converged into a different local minimum. In Figure 4 an easy assignable set of doublets, originating by tunneling rotation interaction, of *R*-type *a*-type transitions with $J' - J'' = 26 - 25$ is shown. Complications arose for transitions with $K_a = 12$, which should not be affected by Coriolis-type interactions. Here, the dataset could not be fit to the experimental uncertainties for $J > 38$, even though more transitions

Table 2: Spectroscopic parameters[a] (MHz) of the two substates for the ground state of *gauche*-propanal.

Parameter	X	ΔX
E		237.7953 (98)
A	26250.6640 (148)	2.0345 (63)
B	4314.92050 (117)	−0.030328 (159)
C	4148.01846 (117)	−0.107072 (90)
Δ_K	2.1000 (41)	−0.008057 (282)
Δ_{JK}	−0.1794215 (84)	0.00046067 (241)
$\Delta_J \times 10^3$	6.58936 (136)	−0.008402 (64)
$d_1 \times 10^3$	1.08232 (88)	−3.922 (33)
$d_2 \times 10^6$	−38.36 (41)	1.4260 (195)
$H_{KJ} \times 10^6$	9.613 (70)	1.3617 (240)
$H_{JK} \times 10^6$	−3.3404 (164)	−0.02918 (69)
$H_J \times 10^9$	127.294 (252)	0.3408 (245)
$h_1 \times 10^9$	−52.463 (193)	−0.8260 (54)
$h_2 \times 10^9$	−0.463 (40)	0.4434 (48)
$h_3 \times 10^9$	−0.1814 (181)	−0.09859 (125)
$L_{KKJ} \times 10^9$	−4.318 (220)	−1.693 (66)
$L_{JK} \times 10^9$	−2.263 (73)	0.02756 (235)
$L_{JJK} \times 10^{12}$	145.05 (216)	−2.580 (101)
$L_J \times 10^{12}$	−3.248 (33)	0.0706 (32)
$l_1 \times 10^{12}$	2.1031 (150)	–
$P_{JK} \times 10^{12}$	−0.1243 (34)	–
$P_J \times 10^{15}$	0.07098 (299)	–
F_{bc}	23.9491 (67)	
F_{bc_K}	−0.1018 (49)	
$F_{bc_J} \times 10^3$	−3.3778 (62)	
$F_{bc_{KK}} \times 10^3$	0.23517 (244)	
$F_{bc_{JK}} \times 10^6$	−14.565 (160)	
$F_{bc_{JJ}} \times 10^6$	0.14996 (76)	
$F_{2bc} \times 10^3$	−0.3618 (39)	
no. of lines	1685	
no. of transitions	2378	
rms error[b]	0.97	

[a]Watson's *S* reduction was used with SPFIT in the I^r-representation. Parameters were fit as linear combinations $X = (X^+ + X^-)/2$ and $\Delta X = (X^+ - X^-)/2$. Values of F_{bc} etc., given between two columns, are associated with operators between both tunneling states; ΔX is not defined for these parameters. Numbers in parentheses are one standard deviation in units of the least significant figures.
[b]Weighted unitless value for the entire fit.

can be assigned securely still straightforwardly (517 in total). The strong lines in Fig. 4 illustrate the possibility of secure assignments to higher K_a quantum numbers, up to $K_a = 22$. The observed deviations could originate from insufficiencies in our spectroscopic model or from interactions with other states, for example the first excited aldehyde torsion of *gauche*, and are shown exemplary for $K_a = 12$ in the supplementary material. The analysis of this excited state is beyond the scope of the present work, but is intended for a future study. A model with assigned and fitted *a*-type transitions up to $J = 60$ and $0 \le K_a \le 13$, except for $J > 50$ for $K_a = 11$ and $J > 38$ for $K_a = 12$, is now available. Additionally, transitions for lower J's up to 31 with K_a up to 17 are included as far as the RMS error was not increasing considerably. Our best choice of rotational and Coriolis interaction parameters for *gauche* is listed in Table 2.
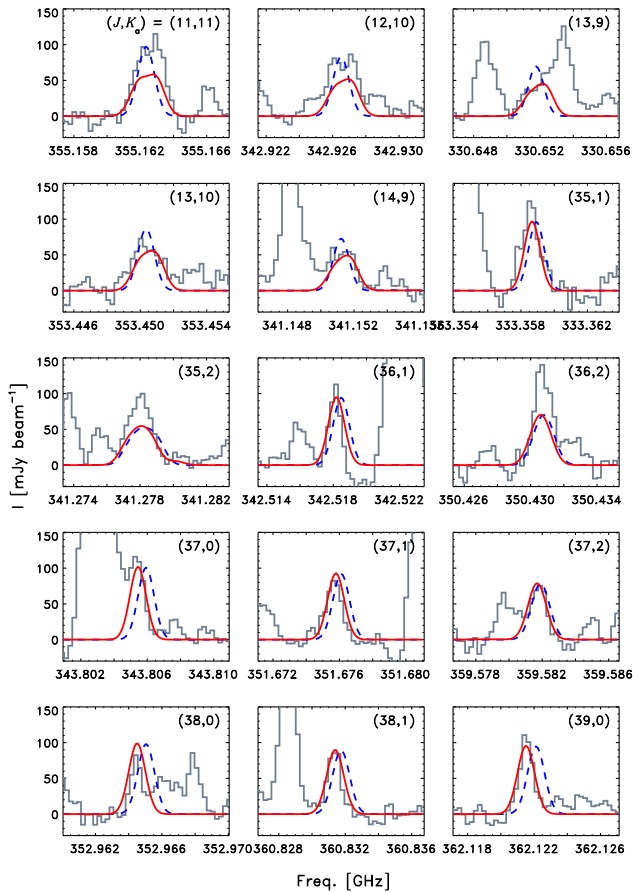
Figure 5: Sections of the ALMA-PILS radio astronomical spectrum toward a position offset from one of the components in the protostellar binary (see Refs. [14] and [15] for details) displaying selected emission features of propanal. The observed spectrum is shown in solid gray lines, the initial model is indicated by dashed blue lines, and the new model by solid red lines. The upper state J and K_a values of the transitions are indicated. The high-K_a, low-J transitions are b-type R-type transitions with unresolved asymmetry splitting, the high-J, low-K_a transitions are blends of two a-type and two b-type R-type transitions which all have $K_c = J - K_a$, where K_a is the lower one of two and the one shown.

4. Discussion and conclusion

The ground and first excited aldehyde torsion of *syn* can be assigned and modeled quite straightforwardly. The improvement of centrifugal distortion constants leads to faithful predictions even in higher frequency regions. The description of these states with a total of 15374 newly assigned and fitted transitions provides satisfactory synthetic spectra for state-of-the-art astronomical observation standards. Only predictions for b-type transitions with K_a quantum numbers much higher than implemented in the fit should be treated with caution, see subsection 3.1.2.

Parameters describing the first excited methyl torsion are quite different compared to the other two states. Since it was treated as an isolated state, but there is evidence that it is perturbed, the model is adequate only for transitions with quantum numbers implemented in the fit. Varying magnitudes of the observed splittings due to internal rotation of the methyl group for the various studied states can be explained roughly with the classical tunneling scheme: Higher relative energies of vibrationally excited states, consequently, smaller energy differences to the potential barrier height of $793.7\pm2.5\,\mathrm{cm}^{-1}$ lead in general to larger splittings. This results in increasing magnitude of the energy tunneling parameter ϵ_{10}, from the ground state $\epsilon_{10} = -3.0941\,(57)\,\mathrm{MHz}$ ($E_{rel} = 0\,\mathrm{cm}^{-1}$) to the first aldehyde torsion $\epsilon_{10} = 38.7984\,(68)\,\mathrm{MHz}$ ($E_{rel} = 135.1\,\mathrm{cm}^{-1}$) up to the first excited methyl torsion $\epsilon_{10} = 130.5541\,(250)\,\mathrm{MHz}$ ($E_{rel} = 219.9\,\mathrm{cm}^{-1}$).

Modelling of *gauche* is somewhat more difficult. Most of the lines can be assigned confidently, but the treatment, even with Coriolis interaction, seems insufficient. The large residuals may be caused by perturbations caused by a yet unidentified state. Wrong assignments not yet identified could also be an explanation as could be the inadequacy of the effective Hamiltonian, or that the large parameter space causes the fit to not converge into the global minimum. Sometimes the fit is converging and the parameter values are reasonable with different sets of parameters, so the right choice is not obvious, nor unambiguous. Missing b- and c-type transitions may affect the description of the K-level structure, and may, in turn, be a reason for our inability to determine F_{ac} with confidence. The magnitude of F_{ac} may well be larger than that of F_{bc}, as, for example, in ethanethiol [24] or hydroxyacetonitrile [25]; see also the theoretical treatment of the reduced axis system [22]. The omission of F_{ac} may influence the ability to determine higher order parameters or affect their values. Complications by describing molecules with two stable degenerate forms and necessary treatment of Coriolis interactions occurred already before [26, 27]. For conformer I of cyanoacetaldehyde only transitions up to $K_a = 2$ for 0^+ and up to $K_a = 8$ for 0^--state are employed in the fit and moreover transitions with J equal to 30, 31, and 32 needed to be excluded [26]. For *synclinal* mercaptoacetonitrile, the standard deviation is four times larger than the expected experimental uncertainty and again special kinds of transitions were excluded, regarding large deviations between experimental and calculated frequencies [27]. For *gauche* propanal, a first model is now available into the submillimeter wave region.

This extensive study of propanal could lead to a better understanding of the behavior of complex molecules with two large amplitude motions, here originating from its two functional groups, the aldehyde and methyl groups.

With the newly derived constants of this work the synthetic spectra of *syn* and *gauche* should satisfy the requirements in sensitivity and accuracy of astronomical observations nowadays, even for warm environments. We have modeled the propanal emission lines with the new predictions and compare them with those previously available. As can be seen in Fig. 5 (*b*-type) transitions with high K_a and low J appear weaker, broader, and slightly shifted because of the consideration of the methyl internal rotation in the present predictions. Overprediction of line intensities does not occur anymore. Transitions with high J and low K_a, on the other hand, are shifted by up to half a line-width; whenever the shift is large, the agreement is much better with the new predictions.

Predictions of the rotational spectra of *syn*- and *gauche*-propanal are available in the catalog section[1] of the CDMS [28, 29]. In addition, line, parameter, and fit files, along with other auxiliary files, are available in the spectroscopy data section[2] of the CDMS.

Acknowledgments

Appendix A. Supplementary Material

Supplementary data associated with this article can be found, in the online version, at http://dx.doi.org/10.1016/j.jms.2017.07.008.

References

[1] S.S. Butcher, E.B. Wilson Jr., J. Chem. Phys. 40 6 (1964) 1671−1678.

[2] H.M. Pickett, D.G. Scroggin, J. Chem. Phys. 61 10 (1974) 3954−3958.

[3] J. Randell, J.A. Hardy, A.P. Cox, J. Chem. Soc., Faraday Trans. 2, 84 8 (1988) 1199−1212.

[4] J.R. Durig, D.A.C. Compton, A.Q. McArver, J. Chem. Phys. 73 2 (1980) 719−724

[5] G.A. Guirgis, B.R. Drew, T.K. Gounev, J.R. Durig, Spectrochim. Acta A 54 (1998) 123−143.

[6] J.A. Hardy, A.P. Cox, E. Fliege, H. Dreizler, Z. Naturforsch. 37a (1982) 1035−1037.

[7] J. Randell, A.P. Cox, H. Dreizler, Z. Naturforsch. 42a (1987) 957−962.

[8] J. Demaison, H. Maes, B.P. vanEijck, G. Wlodarczak, J. Mol. Spectrosc. 125 (1987) 214−224.

[9] J. Randell, A.P. Cox, K.W. Hillig, M. Imachi, M.S. LaBarge, R.L. Kuczkowski, Z. Naturforsch. 43a (1988) 271−276.

[10] L.E. Snyder, D. Buhl, B. Zuckerman, P. Palmer, Phys. Rev. Lett. 22 (1969) 679−681.

[11] C.A. Gottlieb, M.A. Gordon, L.E. Snyder, Wiley-Interscience New York (1973) 181−186.

[12] J.M. Hollis, P.R. Jewell, F.J. Lovas, A. Remijan, H. Møllendal, Astrophys. J. 610 (2004) L21−L24.

[13] M.A. Requena-Torres, J. Martín-Pintado, S. Martín, M.R. Morris, Astrophys. J. 672 (2008) 352−360.

[14] J.K. Jørgensen, M.H.D. van der Wiel, A. Coutens, J.M. Lykke, H.S.P. Müller, E.F. van Dishoeck, H. Calcutt, P. Bjerkeli, T.L. Bourke, M.N. Drozdovskaya, C. Favre, E.C. Fayolle, R.T. Garrod, S.K. Jacobsen, K.I. Öberg, M.V. Persson, S.F. Wampfler, Astron. Astrophys. 595 (2016) A117.

[15] J.M. Lykke, A. Coutens, J.K. Jørgensen, M.H.D. van der Wiel, R.T. Garrod, H.S.P. Müller, P. Bjerkeli, T.L. Bourke, H. Calcutt, M.N. Drozdovskaya, C. Favre, E.C. Fayolle, S.K. Jacobsen, K.I. Öberg, M.V. Persson, E.F. van Dishoeck, S.F. Wampfler, Astron. Astrophys. 597 (2017) A53.

[16] M.A. Martin-Drumel, J. van Wijngaarden, O. Zingsheim, F. Lewen, M.E. Harding, S. Schlemmer, S. Thorwirth, J. Mol. Spectrosc. 307 (2015) 33−39.

[17] Virginia Diodes, Inc. (VDI); address: 979 Second Street, S.E. Suite 309, Charlottesville, VA 22902-6172, USA

[18] P. Groner, J. Chem. Phys. 107 (1997) 4483−4498.

[19] I. Kleiner, J. Mol. Spectrosc. 260 (2010) 1−18.

[20] P. Groner, S. Albert, E. Herbst, F.C. De Lucia, Astrophys. J. 500 (1998) 1059−1063.

[21] H.M. Pickett, J. Mol. Spectrosc. 148 (1991) 371−377.

[22] H.M. Pickett, J. Chem. Phys. 56 (1972) 1715−1723.

[23] D. Christen, H.S.P. Müller, Phys. Chem. Chem. Phys. 5 (2003) 3600−3605.

[24] H.S.P. Müller, A. Belloche, L.-H. Xu, R.M. Lees, R.T. Garrod, A. Walters, J. van Wijngaarden, F. Lewen, S. Schlemmer, K.M. Menten, Astron. Astrophys. 587 (2016) A92.

[25] L. Margulès, B.A. McGuire, M.L. Senent, R.A. Motiyenko, A. Remijan, J.C. Guillemin, Astron. Astrophys. (2017), in press, doi: 10.1051/0004-6361/201628551.

[26] H. Møllendal, L. Margulès, R.A. Motiyenko, N.Wessel Larsen, J.-C. Guillemin, J. Phys. Chem. A 116 (2012) 4047−4056.

[27] H. Møllendal, S. Samdal, J.-C. Guillemin, J. Phys. Chem. A 120 (2016) 1992−2001.

[28] H.S.P. Müller, S. Thorwirth, D.A. Roth, G. Winnewisser, Astrophys. 370 (2001) L49−L52.

[29] H.S.P. Müller, F. Schlöder, J. Stutzki, G. Winnewisser, J. Mol. Struct. 742 (2005) 215−227.

---

[1] https://cdms.astro.uni-koeln.de/classic/entries/

[2] https://cdms.astro.uni-koeln.de/classic/predictions/daten/CH3CH2CHO/